A Characterization Of Volatile Organic Compounds And Secondary Organic Aerosol At A Mountain Site In The Southeastern United States

By: Michael Link, Yong Zhou, Brett Taubman, **James Sherman**, Hadi Morrow, Ian Krintz, Luke Robertson, Ryan Cook, Justine Stocks, Matthew West, and Barkley C. Sive

Abstract

Mean temperature anomalies in the Southeastern United States (SEUS) over the past century have reflected regional cooling hypothesized to be a result of an enhancement of warm season aerosol optical thickness caused by the oxidation of biogenic volatile organic compounds (VOCs). Aerosol and gas-phase VOC measurements were made at the Appalachian Atmospheric Interdisciplinary Research (AppalAIR) site in the southern Appalachian mountains of North Carolina during the summer of 2013 in an effort to characterize warm season chemistry. Organic aerosol (OA) chemistry was characterized through a positive matrix factorization analysis resolving a low-volatility, semi-volatile, and isoprene oxidation factor contributing 34±15, 24±12, and 42±17 %, respectively to the total observed OA. Volatile organic compound characterization described chemistry that was typical of rural background levels with periods of elevated hydrocarbon and urban tracer loading that varied with synoptic flow. Chemical, meteorological, and aerosol optical property data suggested that measurements made at the AppalAIR site are representative of background atmospheric chemistry in the SEUS. Annual background secondary organic aerosol (SOA) production in the SEUS was estimated to be 0.15–0.50 GgC yr−1. Estimates of total and background SOA from this study provide evidence that the SEUS is a region of global significance in the context of global SOA budgets, and can be useful in understanding the extent of anthropogenic enhancement of summertime SOA compared to background levels.

Link, M., Zhou, Y., Taubman, B. et al. A characterization of volatile organic compounds and secondary organic aerosol at a mountain site in the Southeastern United States. J Atmos Chem (2015) 72: 81. https://doi.org/10.1007/s10874-015-9305-5. Publisher version of record available at: https://link.springer.com/article/10.1007/s10874-015-9305-5

A characterization of volatile organic compounds and secondary organic aerosol at a mountain site in the Southeastern United States

Michael Link[1] · **Yong Zhou**[2] · **Brett Taubman**[1] · **James Sherman**[3] · **Hadi Morrow**[1] · **Ian Krintz**[3] · **Luke Robertson**[3] · **Ryan Cook**[1] · **Justine Stocks**[1] · **Matthew West**[3] · **Barkley C. Sive**[4]

Abstract Mean temperature anomalies in the Southeastern United States (SEUS) over the past century have reflected regional cooling hypothesized to be a result of an enhancement of warm season aerosol optical thickness caused by the oxidation of biogenic volatile organic compounds (VOCs). Aerosol and gas-phase VOC measurements were made at the Appalachian Atmospheric Interdisciplinary Research (AppalAIR) site in the southern Appalachian mountains of North Carolina during the summer of 2013 in an effort to characterize warm season chemistry. Organic aerosol (OA) chemistry was characterized through a positive matrix factorization analysis resolving a low-volatility, semi-volatile, and isoprene oxidation factor contributing 34±15, 24±12, and 42±17 %, respectively to the total observed OA. Volatile organic compound characterization described chemistry that was typical of rural background levels with periods of elevated hydrocarbon and urban tracer loading that varied with synoptic flow. Chemical, meteorological, and aerosol optical property data suggested that measurements made at the AppalAIR site are representative of background atmospheric chemistry in the SEUS. Annual background secondary organic aerosol (SOA) production in the SEUS was estimated to be 0.15–0.50 GgC yr^{-1}. Estimates of total and background SOA from this study provide evidence that the SEUS is a region of global significance in the context

✉ Michael Link
linkmf@rams.colostate.edu

[1] Department of Chemistry, Appalachian State University, Boone, NC 28608, USA

[2] Department of Atmospheric Science, Colorado State University, Fort Collins, CO 80523, USA

[3] Department of Physics, Appalachian State University, Boone, NC 28608, USA

[4] Air Resources Division, National Park Service, Lakewood, CO 80235, USA

of global SOA budgets, and can be useful in understanding the extent of anthropogenic enhancement of summertime SOA compared to background levels.

Keywords Secondary organic aerosol · Southeastern United States · Positive Matrix Factorization · Aerosol mass spectrometry

1 Introduction

Significant uncertainties currently exist in global climate models, in part, resulting from a limited understanding of the action of aerosol direct and indirect effects on the climate (Hallquist et al. 2009; IPCC 2013). It has become known in recent years that organic aerosols (OA) constitute a significant fraction of total condensed-phase material in the atmosphere globally, and thus may serve a pivotal role in regulating global climate (Zhang et al. 2007a, b; Jimenez et al. 2009; Slowik et al. 2010). The exact influence of OA on regional and global climates remains uncertain not only because of their varied chemical compositions and physical properties, but also because estimates of total OA loading to the atmosphere can be highly variable (Ford and Heald 2013). The global OA budget is composed of contributions from primary OA (POA), emitted from point sources and relatively short-lived in the atmosphere, as well as secondary OA (SOA) that is formed from nucleation processes, oxidation reactions, heterogeneous and aqueous chemistry, and may ultimately represent the fraction of OA with a significant influence in climate regulation (Kanakidou et al. 2005; Carlton and Baker 2011).

Goldstein et al. (2009) suggested that a "cooling haze", composed of secondary organic aerosol (SOA), in part caused by the influence of anthropogenic seed aerosol on the oxidation of biogenic volatile organic compounds (BVOCs), is formed over the southeastern United States (SEUS) during warm season months and is responsible for negative aerosol direct radiative forcing at the top of the atmosphere during these months. In the past, isoprene has not been considered to contribute as significantly to SOA production relative to monoterpenes and sesquiterpenes (Liousse et al. 1996; Griffin et al. 1999; Kanakidou et al. 2005; Henze et al. 2006); however, other studies have found that isoprene can dominate regional VOC reactivity in rural areas and its oxidation products may constitute more than 50 % of the measured SOA mass (Riemer et al. 1998; White et al. 2008) in rural areas. An increasingly thorough method for the characterization of SOA resulting from isoprene oxidation, including markers suggesting anthropogenic SOA enhancement, has recently been developed (Claeys et al. 2004; Lin et al. 2013). Surratt et al. (2007a, b, 2010) were the first to identify unique isoprene oxidation intermediates, such as isoprene epoxydiols (IEPOX), that form in both high nitrogen oxide (NO_x=NO_2+NO) and low-NO_x environments, which increased the general understanding of how aerosol acidity and atmospheric sulfuric acid play roles in isoprene oxidation chemistry. Additionally, OA that has similar mass spectral signatures to IEPOX has been identified as constituting the dominant fraction (33 %) of observed OA at an urban site in the SEUS (Budisulistiorini et al. 2013). Emerging studies such as these demonstrate that sources of biogenic SOA, particularly related to isoprene oxidation, could have significant influence in global climate regulation (Carlton and Baker 2011; Robinson et al. 2011; Pye et al. 2013).

Currently, models account for the global atmospheric SOA burden and production through two methods; bottom-up and top-down approaches (Goldstein and Galbally 2007; Heald et al. 2010; Spracklen et al. 2011). The bottom-up approach uses known or inferred VOC precursor

fluxes combined with laboratory data to estimate global SOA production at 50–90 TgC yr^{-1}. The top-down method uses atmospheric SOA measurements to constrain the fate of all VOC precursor fluxes to SOA resulting in an estimate of 140–910 TgC yr^{-1} (Hallquist et al. 2009). These discrepancies exist not only because of the differences between observed yields of SOA from VOC oxidation in the laboratory and expected yields modeled in the ambient environment, but are also influenced by complex SOA formation mechanisms such as the "enhanced" production of biogenic SOA (eBSOA) suggested to be catalyzed by anthropogenic pollutants such as sulfur dioxide (SO_2), NO_x, and acidic seed aerosol (Hoyle et al. 2011). Recent modeling work has suggested that approximately 50 % of observed SOA in the SEUS is a formed as a result of the oxidation of isoprene (Liao et al. 2007), some of which is anthropogenically influenced (Spracklen et al. 2011), so a background SOA estimation based on measurements that constrain contributing variables provides context into which eBSOA can be understood and estimated for the SEUS. Uncertainty in the extent of eBSOA production demonstrates the importance of performing studies of ambient aerosol to not only reconcile differences between measurements and models, but also to characterize major observable contributions of anthropogenic input on the production of SOA. Additionally, with robust estimates of SOA loading, or typical regional "background" fluxes, models can be further constrained and used for the purpose of refining regional to global radiative forcing estimates.

The goal of this study was not only to characterize ambient aerosol and VOCs in a high-elevation rural environment in the SEUS, but also to formulate an empirical estimate of "background" SOA based on measurements made at a sampling site where the observed atmospheric chemistry was regionally representative of the SEUS. Using concurrent aerosol and gas-phase chemical measurements, this study characterizes SOA factors representative of regional background SOA in the SEUS. These measurements are used to estimate annual background SOA for the SEUS which could be useful for characterizing organic aerosol at other sites in the SEUS such as those represented by the Southeastern Aerosol Research and Characterization network (Hansen et al. 2003; Gao et al. 2006). This work presents data that suggests a common mechanism controlling isoprene oxidation and SOA formation in the rural SEUS, and provides a basis for which anthropogenically enhanced SOA formation in the SEUS can be understood from the context of a regional estimate of background SOA.

2 Methods

2.1 Sampling period description

All measurements were made on the campus of Appalachian State University in Boone, NC (36.21°N, 81.69°W, elevation 1100 m asl) at the Appalachian Atmospheric Interdisciplinary Research facility (AppalAIR). The aerosol sampling line was identical to that described in Kelly et al. (2012). Aerosol was sampled from a 34-m tower at AppalAIR that protrudes above the surrounding forest canopy. The sampling flowrate into the main stack was 1000 L min^{-1} from which 150 L min^{-1} was diverted to five individual stainless steel sampling lines (30 L min^{-1} each) within the facility. Sampling lines were heated at two points to keep air samples at a relative humidity of less than 40 %. Air for VOC measurements was continuously drawn through a 3/8-inch O.D. Teflon sampling line at a rate of 14 L min^{-1} from the top of the tower.. The AppalAIR facility is located at one of the highest points in Boone, and is near a crest of the southern Appalachian Mountains. As a result of its location, AppalAIR is exposed

to synoptic flow on all sides. The AppalAIR site is a forested site in which the dominant tree species are deciduous varieties such as oak, birch and ash with some contributions of coniferous trees such as fraser fir and red spruce. Aerosol chemical measurements were acquired from December 19, 2012 to March 28, 2013, to represent the winter of 2013; and June 3 to July 31, 2013, to represent the summer of 2013. VOC measurements were made from June 15 to July 2, 2013.

2.2 Instrumentation

An Aerodyne quadrupole aerosol mass spectrometer (AMS) was used to measure size-resolved mass distributions and mass loadings of non-refractory chemical components of sub-micrometer particles, including organics, sulfate, nitrate, and ammonium (Jayne et al. 2000; Jimenez et al. 2003; Canagaratna et al. 2007). The AMS consists of three major components: a particle beam generation inlet system, an aerodynamic sizing chamber, and a particle composition detection section. Aerosol particles enter the AMS through a 130 μm critical orifice which limits the flow rate to ~150 ml/min. The particles are focused into a narrow beam (<1 mm diameter) using an aerodynamic focusing lens (Liu et al. 1995a, b). The particle beam travels across the vacuum sizing chamber, passes through a chopper for information on particle time of flight, and is directed onto a resistively heated surface, where non-refractory chemical components of particles are vaporized and ionized with a 70 eV electron impact ionization source. The fragment ions are analyzed with a quadrupole mass spectrometer.

The AMS was operated in mass spectrum (MS)/particle time-of-flight (TOF) alternate mode, however only data collected from the MS mode are reported here In the MS mode, the AMS scanned the entire m/z range from 1 to 300 amu at 1 ms/amu with resolution of 1 amu, providing mass loading of all fragment ions less than 301 amu. Data for the mass concentrations were averaged to 10 min. Calibrations were performed on site before the sampling period and during the sampling period when the MS air beam signal decreased to 70 % of the reference value established at Aerodyne. Calibrations were performed using monodisperse ammonium nitrate aerosols generated by an atomized solution dried in a diffusion dryer.

From June 15 to July 2, 2013, whole air grab samples were collected hourly in 2-L electropolished stainless steel canisters which were pressurized to 30 psig using a single head metal bellows pump (MB-302, Senior Aerospace, Sharon, MA). In total, 408 hourly canister samples were collected from June 15 to July 2, 2013. Canister samples were returned to the laboratory at Appalachian State University in Boone, NC and analyzed for a comprehensive suite of VOCs. All samples were analyzed soon after the sampling period such that every sample was analyzed within 1 week of sample collection. A total of 90 individual VOCs were quantified from the canister samples using a five-channel, three gas chromatograph (GC) analytical system that consisted of two flame ionization detectors (FIDs), two electron capture detector (ECDs) and one mass spectrometer (MS). The gases measured included C_2-C_{10} nonmethane hydrocarbons (NMHCs), C_1-C_2 halocarbons, C_1-C_5 alkyl nitrates, reduced sulfur compounds, and oxygenated VOCs (OVOCs) (Zhou et al. 2005). The analytical system and methodology used for this study are similar to those used in previous studies (Sive 1998; Zhou et al. 2010; Russo et al. 2010). The measurement precision, represented by the relative standard deviation (RSD) of the peak areas for each compound in the whole air standards, was 3–15 % for halocarbons, 1–8 % for the NMHCs, 3–8 % for the alkyl nitrates, 3–5 % for the sulfur compounds and 8–10 % for the OVOCs.

2.3 Analytical methods

2.3.1 Positive matrix factorization calculations

Positive Matrix Factorization (PMF) has been applied successfully to AMS organic aerosol datasets in order to characterize observed bulk OA (Lanz et al. 2007; Ulbrich et al. 2009a). The use of this calculation in characterizing the sources of ambient aerosols has been pivotal in elucidating organic aerosol lifetime in the atmosphere as well as anthropogenic influence on SOA formation (Volkamer et al. 2006; Jimenez et al. 2009; Ng et al. 2010), and can be useful in identifying the type of OA most representative of what would be expected of background SOA. PMF calculations were applied to the AMS OA datasets to resolve factors contributing to total observed OA. The structure of the PMF calculation has been extensively described in the literature (Edgerton et al. 2003; Brown et al. 2011; Zhang et al. 2011), and will only be briefly described here. The PMF analysis is a bilinear model that treats the AMS data as a superposition of factors contributing to the total organic mass spectral features and concentration signal observed over time. The mathematical structure of the model is described as $org_{ij} = \sum_{p=1}^{p} ts_{ip} ms_{jp} + e_{ij}$ where org_{ij} is the entire organic data matrix consisting of i rows of time contributions and j columns of mass concentration values, ts_{ip} is the time series contributions from a given factor p, ms_{jp} is the mass concentration contributions from a given factor p, and e_{ij} is the residual data left as a result of the variance in the least-squares fitting for a solution (Paatero and Tapper 1994; Paatero 1999). Solutions were chosen on the basis of mathematical minimizations and physical interpretability (Zhang et al. 2011).

2.3.2 HYSPLIT clustering analysis

Air parcel 120-h backward trajectories were modeled using NOAA's Hybrid Single Particle Lagrangian Integrated Particle (HYSPLIT) model (Draxler 1999) to explore source region contributions to observed chemistry for the summer of 2013. A total of 442 backward trajectories were modeled starting from the coordinates of AppalAIR (38.2°N, 81.7°W), and from a height of 500 m agl every 6 h from the dates of June 1 to August 15, 2013. Back trajectories were grouped into similar source regions using the "clustering" analysis. Choosing a solution to the cluster analysis has been described in detail (Taubman et al. 2006; Hains et al. 2008). The greatest change in total spatial variance was observed from the change to two and six cluster solutions, so the six cluster solution was chosen to be most representative of source regions during the sampling period.

3 Results and discussion

3.1 Distributions of VOCs

The measured VOC distributions were used to generally characterize the relative importance of emission sources affecting the sampling site and to determine time periods representative of regional background atmospheric composition. Characterization of VOC mixing ratios at the AppalAIR site also provides gas phase chemical information into which the observed aerosol chemistry can be put into context.

Variable mixing ratios were observed for the different chemical classes of VOCs during the sampling period as shown by the subtotal ranges in Table 1. Among the eight most abundant VOCs measured in this study were methanol, ethanol, ethane, propane, acetone, isoprene, acetaldehyde, and MVK (Table 1). Mixing ratios of most of the alkanes, alkenes, alkyl nitrates, methanol (MeOH), and ethanol (EtOH) were approximately distributed around the top 90th percentile of the total measurements from June 20–23 (Fig. 1). As a result, summary statistics were calculated for both the entire sampling period, and for the sampling period excluding this 3 day period of elevated mixing ratios. Excluding this 3 day period decreased the RSDs for many compounds suggesting that the observed mixing ratios of VOCs during this period may not be representative of background VOC composition at AppalAIR. The RSDs for biogenic tracers during the entire sampling period, including isoprene; α-pinene; β-pinene; methocrolein (MACR); and methyl vinyl ketone (MVK), were all greater than that of the RSDs for the subtotals of all other chemical classes suggesting that variability in local chemistry is strongly influenced by biogenic emissions.

The OVOCs dominated the distribution of the total measured VOCs (64 %). The mean OVOC mixing ratios observed in this study are consistent with the means of what has been observed at another SEUS rural site (Riemer et al. 1998) and other rural sites in the US (Schade and Goldstein 2001; Karl et al. 2003; Schade and Goldstein 2006; Jordan et al. 2009) during the summer. The most dominant OVOCs, methanol, ethanol, acetaldehyde, and acetone, are known to be secondary products of hydrocarbon oxidation, but many studies also have suggested they have significant biogenic primary sources (Kesselmeier and Staudt 1999; Galbally and Kirstine 2002; Mao et al. 2006; Jordan et al. 2009). The dominance of OVOCs suggests products of photochemistry and/or biogenic emissions have a greater influence on the chemistry of the site than direct urban emission sources.

All C_2-C_6 alkanes comprised 16 % of total measured VOCs by mixing ratio at the site. Mixing ratios of observed alkanes were lower than what has been observed in most major U.S. cities (Baker et al. 2008), but also in some southeastern national parks (Kang et al. 2003). Important tracers for direct urban combustion and fuel evaporation emissions such as ethyne, aromatics, and alkenes were observed to be, on average, several times lower than what has been observed in many U.S. cities suggesting that direct urban emissions have minimal influence on the VOC composition measured at the AppalAIR site. Kang et al. (2003) and references therein reported mixing ratios, of the most dominant anthropogenic NMHCs measured in this study that were often two to three times greater than observed at AppalAIR or at national parks in the SEUS, including Mammoth Cave National Park, KY; Shenandoah National Park, VA; and Great Smokey Mountains National Park, TN. The differences between the values reported in Kang et al. (2003) and values observed at the AppalAIR site may be a result of stricter federal and state regulations such as the Clean Air Act on industrial emissions since the early 2000's. Average magnitude of the mixing ratios of alkanes, alkenes, and aromatics measured in this experiment were within the mean and standard deviation of what was observed during the summer at two rural sites in New Hampshire (White et al. 2008; Russo et al. 2010).

The biogenic hydrocarbons measured the compounds analyzed in this study were limited to α-pinene, β-pinene, and isoprene. Isoprene concentrations rarely exceeded 3 ppbv. Values observed here for isoprene are much smaller than observed in a 1995 study (Kang et al. 2003) that observed mean average mixing ratios of isoprene ranging from 6

Table 1 Summary Statistics of all measured VOCs sampled hourly between June 15–July 2, 2013

Compound	[a]Total Sampling Period Mixing Ratios (pptv)				[b]Mixing Ratios excluding June 20th–June 23rd (pptv)			
	Mean (SD)	Median	Range	% RSD (%)	Mean (SD)	Median	Range	% RSD (%)
[c]Ethane	1.61 (0.78)	1.39	0.75–5.41	48	1.54 (0.85)	1.33	0.75–5.41	54
[c]Propane	0.81 (0.60)	0.64	0.24–4.25	74	0.71 (0.37)	0.63	0.24–3.96	52
i-butane	71 (43)	61	16–398	61	67 (31)	62	16–218	46
n-butane	191 (145)	155	50–1,609	76	171 (75)	155	50–678	44
Cyclopentane	10 (7)	9	1–81	70	10 (6)	9	1–81	60
i-pentane	195 (220)	139	31–2,476	113	154 (100)	133	31–1,067	65
n-pentane	103 (100)	80	10–1,087	97	86 (49)	78	10–534	57
n-hexane	21 (24)	16	1–334	114	18 (21)	16	1–333	118
[c]Total alkanes	2.99 (1.57)	2.57	1.28–12.73	52	2.74 (1.22)	2.45	1.28–8.28	45
Ethene	177 (112)	144	45–917	63	159 (90)	140	45–850	57
Propene	45 (30)	37	7–257	67	41 (25)	36	7–248	60
Trans-2-butene	4 (6)	3	1–58	150	4 (2)	3	1–14	67
1-butene	7 (5)	5	1–38	71	6 (4)	5	1–35	66
i-butene	17 (9)	15	3–74	53	16 (8)	15	3–74	48
Cis-2-butene	5 (15)	2	1–157	300	4 (17)	2	1–157	386
Total alkenes	443 (224)	382	163–1,894	51	225 (108)	201	163–1,216	48
Ethyne	192 (77)	175	63–608	40	172 (54)	161	63–589	31
Benzene	42 (17)	39	1–142	40	39 (13)	37	18–142	33
Toluene	57 (48)	43	13–339	84	46 (29)	39	13–325	64
Ethylbenzene	8 (7)	6	2–59	88	7 (6)	6	2–59	78
m+p-Xylene	19 (20)	13	2–157	105	15 (14)	12	2–157	88
o-Xylene	9 (8)	7	1–66	89	7 (6)	6	1–66	77
Styrene	6 (9)	3	1–118	150	5 (8)	3	1–118	162
n-Propylbenzene	3 (4)	2	1–59	133	3 (4)	2	1–59	150
Total Aromatics	144 (102)	115	42–874	71	121 (68)	106	42–874	56
C_2HCl_3	1.1 (1.3)	0.7	0.2–18.3	121	1.0 (1.3)	0.7	0.2–18.3	135
C_2Cl_4	7.3 (3.9)	6.1	3.4–37.0	53	6.2 (2.4)	5.8	3.4–37.0	39
$MeONO_2$	1.7 (0.4)	1.6	0.7–4.8	23	1.7 (0.4)	1.6	0.8–4.8	24
$EtONO_2$	3.1 (0.8)	3.0	0.8–6.1	26	2.9 (0.7)	2.9	0.8–5.0	24
2-$PrONO_2$	4.6 (1.4)	4.2	2.5–9.3	31	4.4 (1.3)	4.1	2.5–9.3	30
1-$PrONO_2$	1.6 (0.6)	1.5	0.7–4.5	39	1.6 (0.6)	1.4	0.7–4.5	38
2-$BuONO_2$	6.8 (2.8)	6.0	2.9–17.0	42	6.6 (2.9)	5.8	2.9–17.0	44
3-$PenONO_2$	1.9 (0.8)	1.7	0.3–20	42	1.9 (0.8)	1.7	0.6–4.3	41
2-$PenONO_2$	4.0 (2.0)	3.4	0.9–16.4	51.1	3.9 (2.0)	3.3	0.9–16.4	52
Total alkyl nitrates	25.1 (8.7)	22.6	12.0–54.0	34.6	24.3 (8.3)	21.9	12.0–54.0	34
[c]MeOH	2.70 (1.81)	2.27	0.70–12.7	67	2.39 (1.39)	2.08	0.70–12.66	58
[c]Acetaldehyde	0.45 (0.35)	0.39	0.02–2.09	75	0.44 (0.35)	0.39	0.02–2.09	79
EtOH	214 (266)	138	0–2595	124	193 (257)	119	0–2595	133
[c]Acetone	2.32 (0.51)	2.25	1.28–4.51	22	2.31 (0.53)	2.22	1.28–4.51	23
MACR	188 (105)	172	5–679	56	187 (110)	169	5–679	58

Table 1 (continued)

Compound	[a]Total Sampling Period Mixing Ratios (pptv)				[b]Mixing Ratios excluding June 20th–June 23rd (pptv)			
	Mean (SD)	Median	Range	% RSD (%)	Mean (SD)	Median	Range	% RSD (%)
MVK	225 (161)	189	5–999	72	219 (161)	180	5–999	74
MEK	250 (131)	232	53–841	48	251 (126)	229	53–841	50
[c]Total OVOCs	6.33 (2.30)	5.92	0.39–15.70	37	5.96 (2.01)	5.63	0.39–15.63	34
Isoprene	743 (575)	582	1–3,375	77	762 (575)	593	22–3,375	75
α-pinene	23 (18)	20	1–139	78	23 (15)	20	1–139	65
β-pinene	25 (16)	21	1–104	64	24 (14)	21	1–104	57

[a] Summary statistics presented here are for the entire sampling period

[b] Summary statistics presented here are for the entire sampling period excluding 3 days representing a time where polluted air influenced background chemistry from June 20th to June 23rd

[c] Mixing ratios reported in ppbv

to 15 ppbv at SEUS national parks, but fell within the standard deviation of mean values reported from other studies conducted during the summer at rural sites (Reimer et al. 1998; Apel et al. 2002; Jordan et al. 2009). Riemer et al. (1998) reported isoprene mixing ratios between 2-3ppbv for daytime averages during the summer from a rural site in the SEUS. Much of the variability observed in isoprene mixing ratios is a result of its typical temperature dependent emission behavior. In contrast, monoterpenes were observed to have average mixing ratios around 20 pptv with maximum observed values just above 100 pptv. Monoterpenes did not display distinct emission patterns which is expected because their emissions respond to both light and temperature (Bertin et al. 1997; Dindorf et al. 2006). Additionally, monoterpenes will also react with hydroxyl radical and ozone more quickly than isoprene (Seinfeld and Pandis 2006) which may also account for the observed variability in the monoterpene mixing ratios.

Mixing ratios of the halocarbons, tetrachloroethene (C_2Cl_4) and trichloroethene (C_2HCl_3), exhibited variable mixing ratios throughout the campaign as expressed by the %RSD values of 63 %, and 136 %, respectively (Table 1). Tetrachloroethene, a commonly used dry cleaning solvent, degreasing agent, and useful anthropogenic tracer (Simpson et al. 2004), had the highest average mixing ratio of the measured halocarbons peaking around 25.0 pptv on the evening of June 20 (Fig. 1). Trichloroethene, also a byproduct of anthropogenic activity, likely had a high %RSD due to very low observed mixing ratios over the sampling period. This peak C_2Cl_4 mixing ratio is greater than the reported average background northern hemisphere values of 5–10 pptv (Simpson et al. 2004), although the mean value for this study falls within that range (Table 1).

Alkyl nitrates are an important component of rural atmospheric chemistry because they act as reservoir species that can be a significant source of NO_x to NO_x-limited regions (Swanson et al. 2003; Russo et al. 2010). The dominant alkyl nitrates in this study were 2-$BuONO_2$, 2-$PrONO_2$, and 2-$PenONO_2$ with mean mixing ratios of 6.8, 4.6, and 4.0 pptv (Table 1). The average mixing ratio for total C_1-C_5 alkyl nitrates, during the entire sampling period, was 25±10 pptv. The observed levels during this study are similar to what has been observed for alkyl nitrates in semi-rural and rural environments (Blake et al. 2003; Russo et al. 2010).

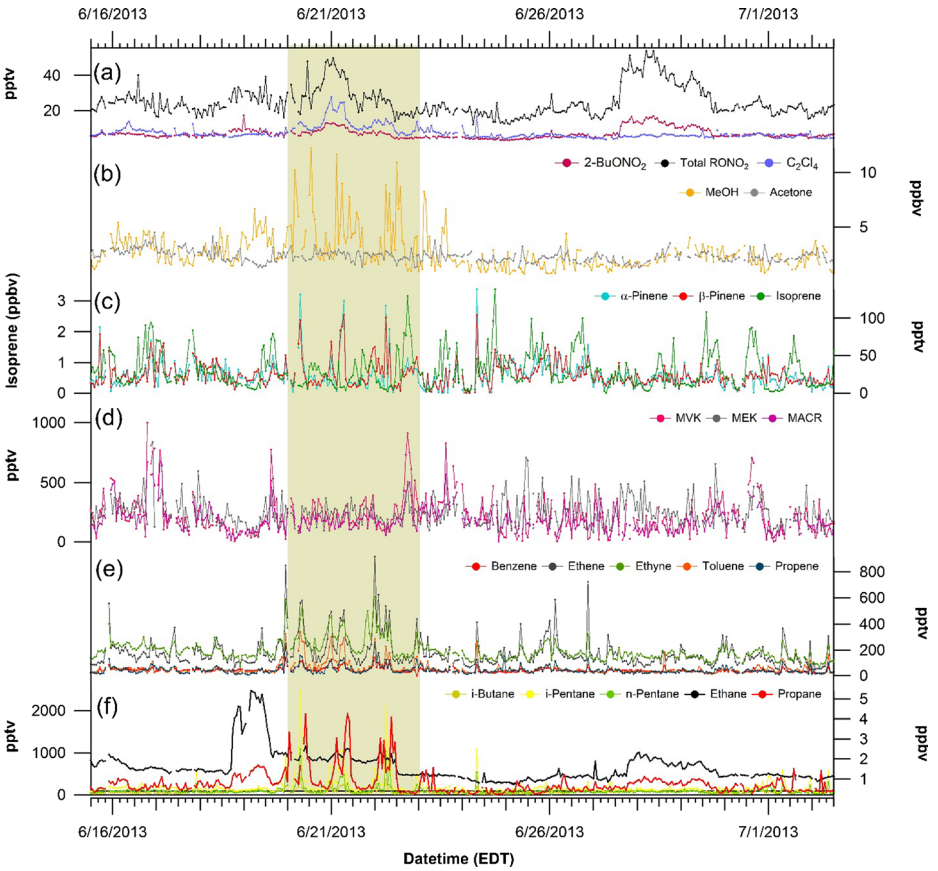

Fig. 1 Time series for selected VOCs measured from June 15–July 2, 2013. The time period between June 20 and 23 (indicated by the *shaded* region) represents the period of pollution where elevated levels of NMHCs and anthropogenic emission tracers were observed. Pictured from *top* to *bottom* is the time series for: **a** 2-butyl nitrate (2-$BuONO_2$), total alkyl nitrates (Total $RONO_2$), tetrachloroethene (C_2Cl_4); **b** methanol (MeOH), ethanol (EtOH); **c** a-pinene, b-pinene, isoprene; **d** methyl vinyl ketone (MVK), methyl ethyl ketone (MEK), methacrolein (MACR), acetaldehyde, acetone; **e** benzene, ethane, ethyne, toluene, propene; **f** ethane, propane, i-butane, n-pentane, i-pentane

Analysis of VOC distributions indicates that the air quality of the AppalAIR site is influenced episodically by regional urban emissions, but on average has the characteristic chemistry of a rural environment with relatively low mixing ratios of non-biogenic NMHCs. Elevated mixing ratios of NMHCs during the period between June 20 to 23 suggests that transport of air masses containing urban emissions originating from backward wind trajectories associated with western air flow may have influenced this period. Some of the most elevated NMHCs such as ethene and propene have atmospheric lifetimes of approximately 1.4 days and 5.3 h, respectively (e.g. Seinfeld and Pandis 2006; White et al. 2008) suggesting that these compounds, as well as some of the longer lived elevated NMHCs such as propane and ethyne, have similar regional sources. The urban emission tracer, C_2Cl_4, also displayed mixing ratio patterns that suggest episodic urban influences. However, mean VOC mixing ratios were similar to other studies of rural environments providing evidence to suggest that VOC chemistry observed at AppalAIR is representative of the regional background a large fraction of the time.

3.2 PMF analysis of AMS data

The PMF calculations were performed for the summer 2013 as well as the winter of 2013. The IGOR PMF GUI v2.06 was used (Ulbrich et al. 2009a). Mass-to-charge ratios (*m/z*) greater than *m/z* 105 were excluded from the PMF calculation because of low signal to noise ratios. A three factor (Fpeak=−0.4) solution for the summer of 2013 (Fig. 2), and a two factor (Fpeak=−0.5) solution for the winter of 2013 (Figure S-2) were chosen as most representative of the chemical composition of ambient OA for these times. Solutions were chosen on the basis of mathematical convergence, stability in the difference between scaled residuals of solutions, factor correlations with reference spectra, characteristic spectral signatures, synoptic influences, and temporal distributions (Zhang et al. 2011). Solutions with a greater number of factors than the ones chosen resulted in factors that either were uncorrelated with reference spectra (Ulbrich et al. 2009a, b, AMS Spectral Database), or included unrealistic spectral features such as the disappearance of m/z 43 or 44. Solutions with less than the number of chosen factors showed evidence of "factor mixing" (Ulbrich et al. 2009a), and were determined to be unrealistic.

The concentration of total measured OA was on average 1.63±1.05 μg m^{-3}. The PMF calculations resolved factors of low-volatility oxygenated OA (LV-OOA), semi-volatile oxygenated OA (SV-OOA), and an isoprene derived OA (Isoprene SOA) that had mass spectral features similar to that of the IEPOX factor for the summer of 2013. Factors comprised on average 35±15, 42±17, and 23±13 % of the submicron OA for LV-OOA, Isoprene SOA, and SV-OOA, respectively (Fig. 3). The LV-OOA factor had the largest m/z 44/43 ratio (Fig. 2), which is characteristic of this factor and indicative of a high degree of oxidation because of the abundance of CO_2^+ (m/z 44) fragments (Aiken et al. 2008). Additionally, this factor correlated very well (r^2=0.98) with LV-OOA reference spectra from the AMS spectral databases as well as the OOA-1 factor (r^2=0.91) from Borneo (Robinson et al. 2011) that was most similar to the

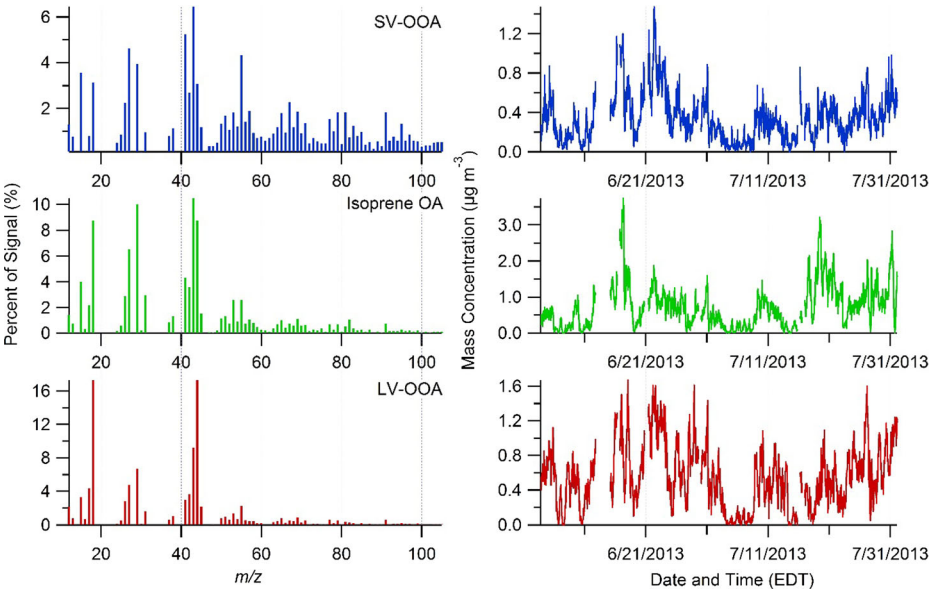

Fig. 2 Time Series and mass spectra for resolved PMF factors from June 3–August 2; SV-OOA (*top panel*), Isoprene OA (*middle panel*), and LV-OOA (*bottom panel*)

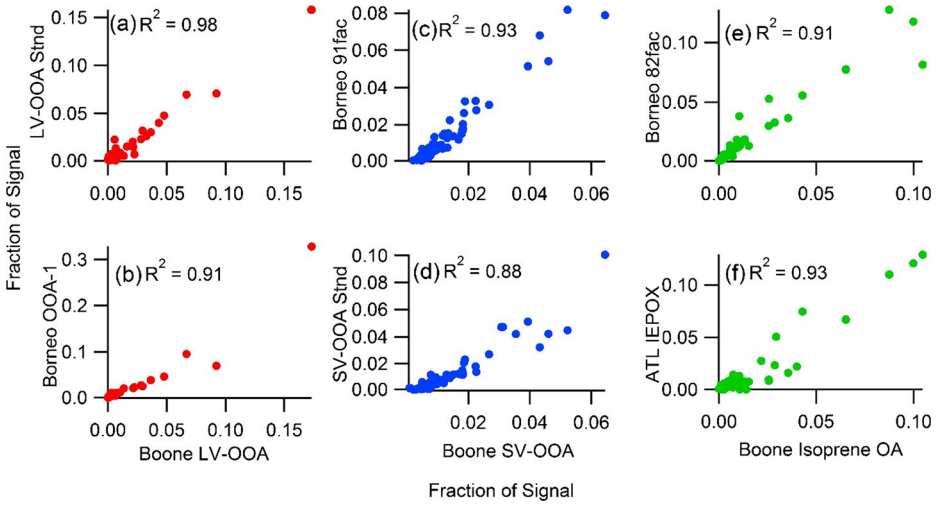

Fig. 3 Resolved Boone PMF factor correlations with select reference spectra from online AMS spectral library (http://cires.colorado.edu/jimenez-group/AMSsd/). Strong correlations include: Boone LV-OOA with the **a** LV-OOA standard [*Ulbrich et al.* 2009a] and **b** Borneo OOA-1 [Robinson et al. 2011]; Boone SV-OOA with the **c** Borneo 91fac [Robinson et al. 2011] and the **d** SV-OOA standard [Ulbrich et al. 2009a]; and Boone Isoprene OA with the **e** Borneo 82fac [Robinson et al. 2011] and the **f** Atlanta IEPOX [Budisulistiorini et al. 2013]

LV-OOA reference. The SV-OOA factor resolved from the Boone dataset correlated well with the reference spectra (r^2=0.88), but had a higher correlation coefficientwith the 91fac (r^2= 0.93) from Borneo. The 91fac from Borneo was suspected to be related to OA from biomass burning, but the exact identity of this factor is not certain because no direct evidence suggesting a relationship between the 91fac and biomass burning was presented when the 91fac was identified in previous work (Robinson et al. 2011). Additionally, there is no known evidence of biomass burning contributing to the summertime OA observed at AppalAIR. The 91fac factor correlates well (r^2=0.84) with the SV-OOA reference spectra suggesting that the spectral characteristics of these factors are chemically similar. The SV-OOA factor observed at the AppalAIR site also exhibits a "picket fence" like fragmentation pattern in which peaks appear at m/z 43, 57, 71, 85 in decreasing abundance (Fig. 2) indicating a fragment in which a $–CH_2^+$ group from a hydrocarbon backbone has been removed. These spectral features support the fact that this factor is of a higher volatility than the LV-OOA factor as a result of the hydrocarbon-like fragmentation (Huffman et al. 2009) which is indicative of a lower oxygen to carbon (O/C) ratio than the LV-OOA factor. The isoprene SOA factor was identified primarily through the appearance of a significant m/z 82 peak in the spectra which has been reported as a tracer for isoprene SOA (Robinson et al. 2011; Budisulistiorini et al. 2013) as well as strong correlations with the IEPOX factor (r^2=0.93) and 82fac (r^2=0.91) from Borneo. The isoprene SOA factor was not identified in the winter dataset which is consistent with predicted low mixing ratios of gas-phase isoprene as a result of temperature dependent emissions.

The results of the PMF calculations for the winter period were more challenging to interpret than the results from the summer dataset. A two-factor solution was chosen to be most representative (Figure S-2) resulting from the correlations of an LV-OOA factor (r^2=0.97, LV-OOA reference spectrum) and a biomass burning OA (BBOA) factor (r^2=0.86, 91fac spectrum and r^2=0.78, BBOA reference spectrum) with reference spectra. Solutions greater than two factors were explored, but resulted in poor correlations and losses in interpretability

of spectral signatures. Similar correlations did result between the two factors with SV-OOA and BBOA reference spectra which suggests that in the two factor solution there may be some mixing of SV-OOA and BBOA factors into one factor. Variability in the episodic emission of BBOA from local sources as well as the spectral similarity of BBOA to SV-OOA further suggests that the BBOA factor in the winter two factor solution may not be as well defined as the LV-OOA factor. However, the LV-OOA factor remained stable through the exploration of four factor solutions suggesting that the identity of this factor, as interpreted, is stable. The appearance of this factor in the summer and winter datasets in similar concentrations suggest that it is representative of background SOA.

3.3 Cluster analysis

Frequency of backward trajectory contributions had an approximately even distribution among all clusters (~20 %) except for the southern (cluster 1) and northern (cluster 6) clusters, whose backward trajectories comprised 10 and 6 % of total modeled trajectories, respectively (Fig. 5). Figure 6 shows the boxplot distributions of the PMF OA factors, as well as selected VOCs, with levels categorized by source region identified by the cluster analysis. Ethane, propane, and the halocarbons showed relatively consistent patterns of mixing ratios across all source regions with the exception of markedly lower mixing ratios of ethane and C_2Cl_4 from the southern cluster. However, tetracholorethene did exhibit a trend of increased mixing ratios originating from the local northern cluster (cluster 5) (Fig. 4) which suggests that this region

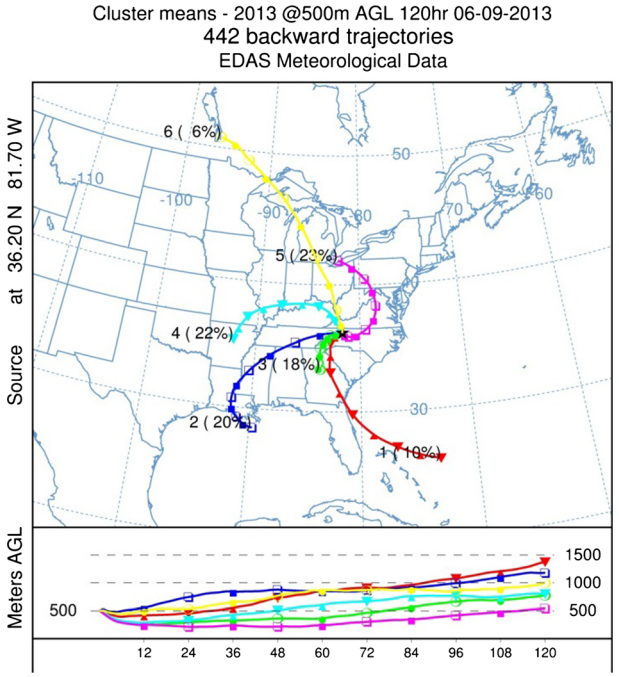

Fig. 4 120-h backward trajectories clustered into source regions for the summer of 2013. Numbered trajectories represent the mean trajectories for each cluster. *1* = south (S), *2* = southwest (SW), *3* = local (Loc), *4* = west (W), *5* = local north (LocN), *6* = north (NW)

may be a source of urban emission transport to AppalAIR. High mixing ratios of isoprene, methanol, and ethanol were associated with the local northern (cluster 5) and western clusters (cluster 4). The highest average mixing ratio of isoprene was associated with the southern cluster (cluster 1). The greatest concentrations of isoprene SOA were associated with the western and local clusters, whereas the concentrations of LV-OOA and SV-OOA only showed slightly greater contributions from the local northern and northwestern clusters. If the 90th and 95th percentiles are considered to be indicators of elevated mixing ratios of isoprene and MVK or elevated concentrations of isoprene SOA, elevated levels of isoprene, MVK, and isoprene SOA have source signatures from regions associated with the LocN and W clusters. The sum of the alkyl nitrates, displayed with the two most abundant alkyl nitrates measured, showed mixing ratios from the southwestern and local northern clusters in which the top 90th percentile of measurements extended to the highest end of the range of observed mixing ratios (Fig. 5). Qualitatively this demonstrated that air masses transported from local north, and occasionally west, are associated with periods of relatively high levels of VOCs and aerosols. These general regions have been characterized by isoprene-rich biogenic VOC emissions (Carlton and Baker 2011) and contributions of anthropogenic pollutants such as sulfur dioxide and particulate matter from fossil fuel production (Goldstein et al. 2009).

3.4 ANOVA analysis

A one-way analysis of variance test (ANOVA) was performed on the chemical and cluster data to determine if patterns of chemical loading had statistically significant association with a particular source region. Least significant difference post hoc tests determined that the loading patterns of compounds observed originating from some source regions were statistically different from others (Table 2). Generally, urban, oil and natural gas, and combustion tracers such as $CHCl_3$, C_2Cl_4, m+p-xylene, toluene, i-pentane, n-pentane, and ethyne showed statistically significant ($p<0.05$) increases associated with the local northern cluster, whose mean trajectory passed over Lake Erie and passed through the Ohio River valley industrial region. This suggests that the Ohio River Valley industrial region may be a source of long-range urban influence to the AppalAIR site. Air masses originating from the southern cluster showed statistically lower mixing ratios of alkyl nitrates than from other source areas. Loading of the Isoprene SOA from the local northern (LocN) showed the highest concentrations that were significantly different from all source regions except from the northern cluster (NW). This suggests that similar production mechanisms for this type of OA may be contributing to the observed concentrations of this OA from these source regions. Although the LV-OOA factor showed a statistically significant pattern of loading from the western cluster, the analysis suggests that the mean value observed from this region was not of the lowest or highest of the observed concentrations so this result does not violate the assertion that loading of this type of OA is relatively homogenous across all source regions.

3.5 Air mass aging using $RONO_2$ kinetics

The age of air masses was investigated to determine the influence of fresh emissions relative to aged emissions using ratios of measured alkyl nitrates to their parent hydrocarbons. This method has been used extensively in other studies (Bertman et al. 1995; Russo et al. 2010; Swarthout et al. 2013). Details of these calculations can be found in the supplement to this manuscript. These calculations were performed for ethyl nitrate ($EtONO_2$), n-propyl nitrate (n-

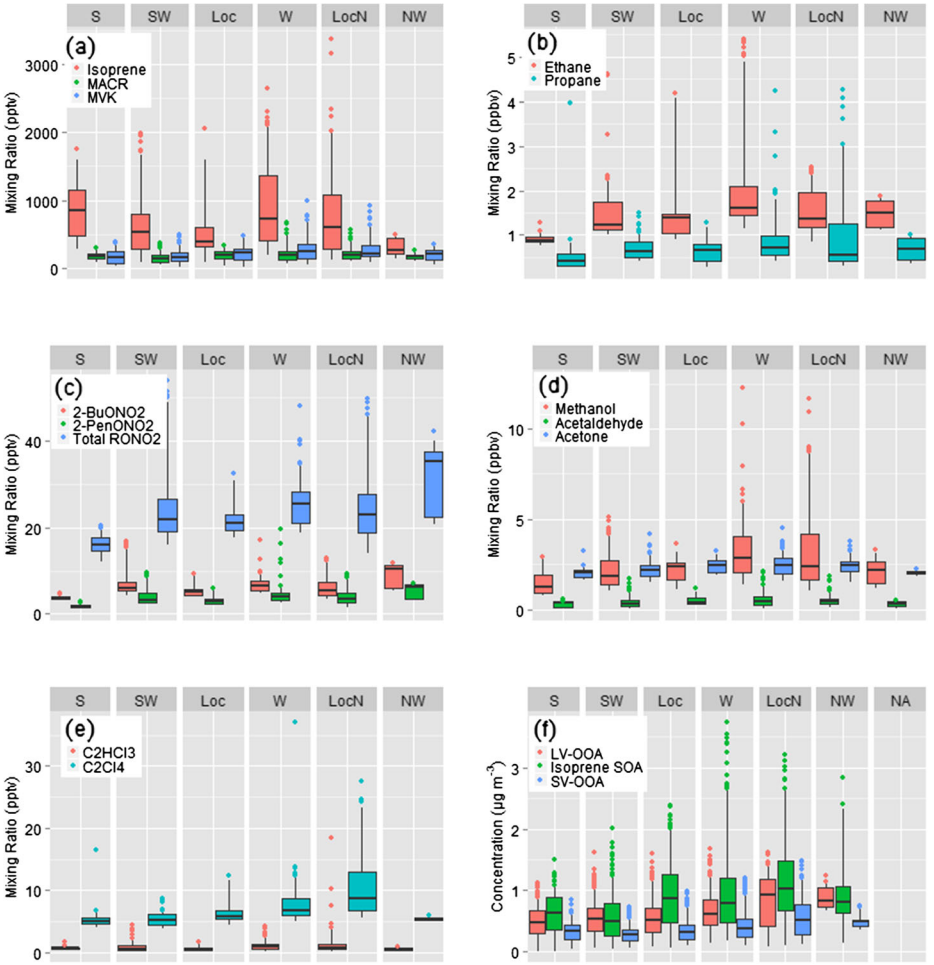

Fig. 5 Aerosol and gas phase chemicals categorized by cluster (Fig. 4). In the box and whisker plots the *solid black line* represents the median, the *top* and *bottom* of the boxes represent the 90th and 10th percentiles, and the *top* and *bottom* whiskers represent the 95th and 5th percentiles, respectively. Represented are: **a** isoprene and isoprene oxidation products, **b** ethane and propane, **c** 2-$BuONO_2$, 2-$PenONO_2$, and total alkyl nitrates, **d** select OVOCs, **e** C_2Cl_4 and C_2HCl_3, and **f** resolved PMF factors

$PrONO_2$), 2-propyl nitrate (2-$PrONO_2$), 2-pentyl nitrate (2-$PenONO_2$), and 3-pentyl nitrate (3-$PenONO_2$), which were all plotted against the ratio of 2-butyl nitrate (2-$BuONO_2$) to its parent hydrocarbon n-butane (Fig. 6). The alkyl nitrates that fit the theoretical curve best were 2-$PrONO_2$ and 2-$PenONO_2$. Despite most of the alkyl nitrates either being aggregated above or below the pure photochemistry curve, the distribution of the data suggest that most of the air masses measured in this study contained compounds that were between 1 and 3 days old, with a small fraction of air masses that were less than a day old and slightly greater than 3 days old. This provides evidence that the AppalAIR site experiences minimal influence from local chemistry and is more influenced by regional transport.

Table 2 Results of the ANOVA analysis of aerosol concentration and VOC mixing ratio variability with source region

Compound	[a]Statistically Different ($p<0.05$) Loading Patterns from All Clusters	[b]Exceptions ($p>0.05$) (main cluster – sub cluster)	[c]Statistically Higher or Lower Loading Patterns from all Clusters
LV-OOA	W		Neither
Isopene SOA	S SW LocN	(S-SW) (LocN-NW)	Neither Neither Higher
SV-OOA	SW		Neither
Ethane	S		Neither
Ethyne	W LocN		Higher Higher
i-Pentane	LocN		Higher
n-Pentane	LocN	(LocN-NW)	Higher
C_2HCl_3	LocN		Higher
C_2Cl_4	LocN		Higher
2-buONO_2	S		Lower
2-penONO_2	S		Lower
Toluene	LocN		Higher
m+p-xylene	LocN		Higher
α-pinene	NW	(NW-Loc)	Lower
β-pinene	NW	(NW-Loc)	Lower

[a] Species that were statistically associated with particular source regions

[b] Non-significant difference of other clusters with the significantly identified cluster

[c] Clusters that were classified as being "neither" higher or lower than the clusters were associated with average concentrations that were in the middle of reported concentration ranges

3.6 Estimating the planetary boundary layer height

In order to calculate total SOA loadings, average summer daytime planetary boundary layer (PBL) heights were computed using 48 individual radiosonde-generated profiles of temperature, relative humidity, and geopotential height during the summer of 2013. Most of the radiosonde sampling occurred for the pre-convective and convective boundary layer, with very little post-convective sampling. Studies have described most, up to 90 % or more, of aerosol mass is contained within the PBL (Heald et al. 2005; Zhang et al. 2007a, b; Ford and Heald 2013), so the measurement of PBL height was considered necessary for calculating background SOA. To determine the PBL height from specific humidity profiles, the location of the negative of the maximum gradient was used, as this indicates the transition to the free troposphere. The slope was computed within a fixed window and iterated with a higher starting height, continuing up throughout the profile (Compton et al. 2013). In addition, the boundary layer height was found from virtual potential temperature profiles using the positive maximum gradient, which is the vertical location of the capping temperature inversion to the PBL (Seidel et al. 2010). Temperature inversions were also specified by the radiosonde software for some profiles and used in PBL height analysis. Average daytime PBL heights and standard deviations (±1σ) over June, July and August produced from the different estimation methods were 1590±588 m agl and 1603±603 m agl for the virtual temperature and specific humidity methods, respectively (Figure S-1). Similarity in the average PBL values and spreads for the virtual temperature and specific humidity methods suggest these two

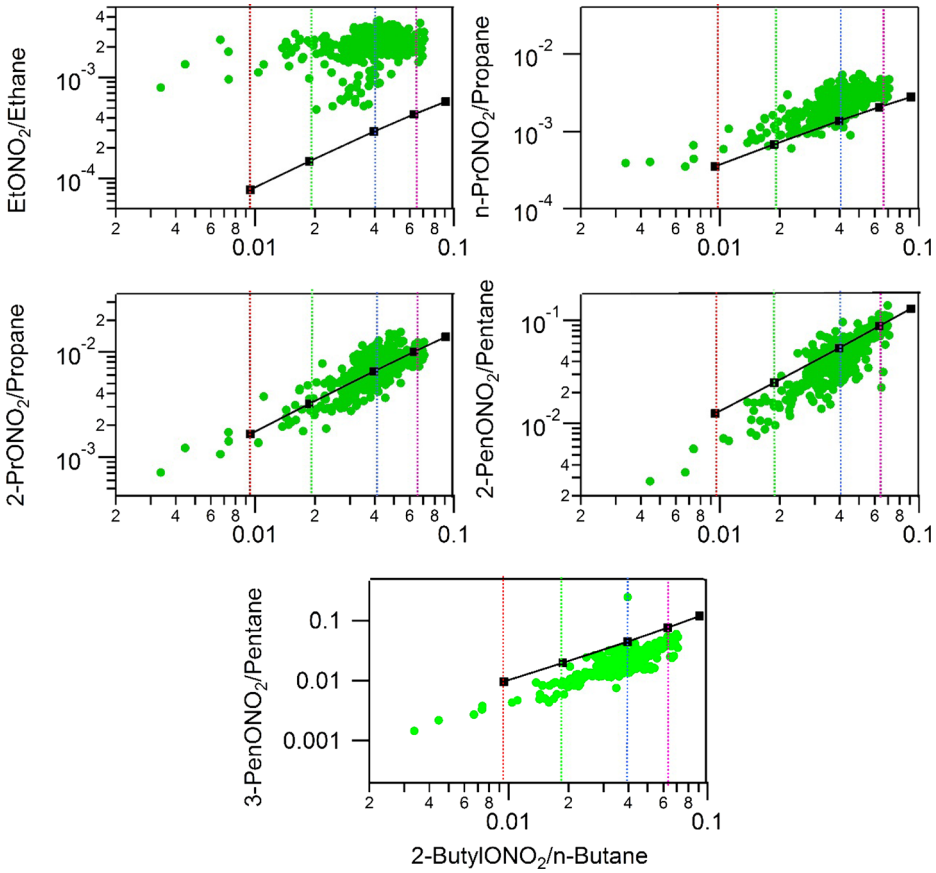

Fig. 6 Alkyl nitrate air mass photochemical aging analysis. Ratios of observed alkyl nitrate to parent hydrocarbons are plotted along a curve (*black dashed line*) that represents the ratios expected of these compounds after a given time of photochemical processing. The *red*, *green*, *blue*, and *purple dashed lines* represent 1, 2, 3 and 4 days of photochemical aging repsepectively. Each alkyl nitrate to parent hydrocarbon ratio is plotted with respect to the most abundent alkyl nitrate, 2-butyl nitrate

methods may produce reliable estimates, so the lowest of the these two values was assumed to be the lower bound on the measured summer daytime PBL height at the AppalAIR site.

3.7 Assessment of regional representation

The AppalAIR site was determined to be regionally representative of the aerosol chemistry of the SEUS based on chemical, synoptic, and optical evidence. The results in Section 3.1 indicated that the VOC chemistry over the summer showed minimal urban influence, and the mixing ratios of many VOCs did not vary significantly. Analysis of chemical concentration patterns with respect to synoptic variability in Section 3.3 also showed that the aerosol and gas-phase chemistry observed during the sampling periods displayed a generally homogeneous distribution across all source regions, with some minor exceptions. Additionally, the alkyl nitrate analysis presented in Section 3.5 suggests that many of the sampled air masses were 1–3 days old, suggesting that regional

transport has a greater impact on VOC chemistry at AppalAIR relative to other sites (Russo et al. 2010; Swarthout et al. 2013). Together, these pieces of evidence suggest that the VOC and aerosol chemistry observed at AppalAIR is mostly representative of the SEUS regional background.

As an additional test of regional representativeness, we applied 8 years of Moderate-resolution Imaging Spectroradiometer (MODIS) AQUA Level 3 globally-gridded aerosol optical depth measurements, (1°×1°) centered above Boone, NC, in addition to quality-assured, daily-averaged temperatures from all SEUS Automated Surface Observing System (ASOS) meteorology sites, obtained from the NC CRONOS (Climate Retrieval and Observations Network of the Southeast Database) database. The first analysis of regional representation sub-divided the SEUS into nine pixels (Fig. 7) each of which were approximately 2°×3° and the aerosol optical depth (AOD) and temperature data was further spatially-averaged at this resolution. Pixel-averaged AOD and daily-averaged surface temperatures for each day over an 8-year period for all days with at least two AOD measurements in a given pixel were correlated according to Eq. 1.

$$AOD(T) = \alpha \exp^{\beta(T-T_o)} \tag{1}$$

The fit parameter α is a measure of aerosol loading (which can vary over the region even if the aerosols are of the same type) while β is a measure of the degree to which the exponential dependence of temperature, T, on AOD holds. This analysis relies on the assumptions that seasonal variability in SEUS aerosol loading is dominated by SOA and that the AOD obeys the same exponential dependence on temperature as BVOC precursor gases (Henze et al. 2006; Goldstein et al. 2009). The degree to which this assumption holds was next determined for each SEUS pixel through a linear regression of ln(AOD) versus $T-T_o$, where α and β are the slope and intercept of the linear regression and T_o= 0 °C. The region over which β and R^2 correlation values were similar to those measured above Boone, NC was estimated to be the area over which AppalAIR aerosol measurements were representative of the regional aerosol type (Table S-1). The correlation and slopes are similar for all nine pixels. The β values for all but pixels 1 and 4 are within 30 % of those reported in previous literature (Goldstein et al. 2009).

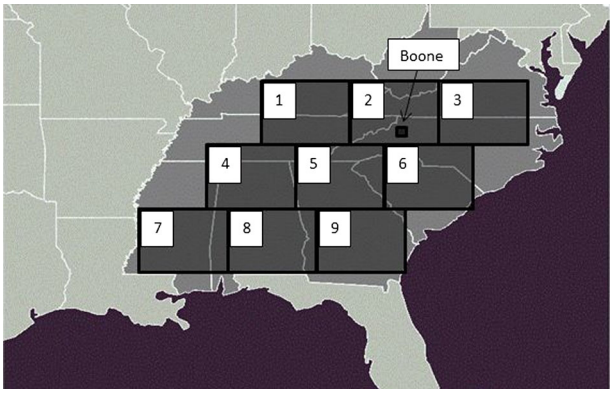

Fig. 7 Numbered pixels (approximately 2°×3°) for which the dependence of AOD on temperature had correlation properties similar to that of the Boone area

3.8 Calculation of the background SOA estimate

The LV-OOA fraction of the total observed OA was used to represent background SOA because of the highly oxidized, "aged" character of this factor. The individual constituents of this factor are generally thought to be processed to the extent that the identification of the origin of the aerosol cannot be determined accurately (Jimenez et al. 2009). Estimates were formulated by first partitioning the SEUS into two volumes by multiplying the constrained area by the measured PBL (Section 3.6), to serve as a lower bound in which SOA would be expected to be contained, as well as an estimated 2.4 km agl PBL, to serve as an upper bound in which SOA would be expected to be contained based on observations from other studies (Morgan et al. 2009; Robinson et al. 2011). Average summer and winter concentrations for the LV-OOA factors were then multiplied by the SEUS volumes. The resultant quantity was ten divided by four estimates of atmospheric lifetime for SOA. Values used for approximate SOA lifetime in this study were 4, 5.4, 8.1, and 11 days based on best estimates in other studies (Kanakidou et al. 2005; Henze and Seinfeld 2006; Henze et al. 2008; Spracklen et al. 2011). Background SOA production rates were then formulated for the summer and winter (Table 3). The conversion between organic matter to organic carbon (OM/OC) was performed using a value of 1.4 (Hallquist et al. 2009). Although recent work (Aiken et al. 2008) has suggested that this value may be less than what has been observed for OA with O/C values (~1.8–2.5) representative of LV-OOA in laboratory experiments, the use of this value suggests that the secondary organic carbon (SOC) estimates provided here might not be as conservative as is suggested by aged SOA composition in the laboratory. Other modeling studies have even used an OA/OC conversion ratio of 2 (Spracklen et al. 2011).

Annual SOA and secondary organic carbon background production estimates are presented in Table 3 averaged for both seasons using the two different PBL height values as well as the range of estimated SOA lifetimes. Average monthly values for both seasons were multiplied by 12 to obtain annual production estimates. The two seasonal monthly estimates of SOC were taken as the ranges for annual background SOC production in the SEUS for a given SOA lifetime (Table 3). The shortest estimated SOA lifetime provided an annual background SOC production range of 0.48–0.58 GgC yr^{-1} and the longest lifetime provided an estimate of 0.18–0.21 GgC yr^{-1}. Most published literature provides global estimates of global SOA production from varied emission or production sources with limited estimates of regional SOA production. To compare the values obtained in this study to reported global SOC values the ratio of the surface area of the SEUS (~6.2×10^4 km^2) to the surface area of the productive land on the earth (~9.9×10^7 km^2) was calculated then multiplied by seven different reported estimates for global SOC production from emission and production sources (Table 3) (Kanakidou et al. 2005; Henze and Seinfeld 2006; Henze et al. 2008; Hallquist et al. 2009; Spracklen et al. 2011). The resulting values provide estimates of SOC production expected for the SEUS based on global SOA literature estimates. Many global SOA models use SOA lifetimes with a median value of 5.4 days (Tsigaridis et al. 2014), and the estimated annual background SOC production range calculated in this study for that aerosol lifetime are slightly higher than what would be expected for the SEUS based on global SOA production from isoprene oxidation (4.4 TgC yr^{-1}) (Henze and Seinfeld 2006) and slightly lower than what would be expected for SOA produced from anthropogenic volatile precursors (8.6 TgC yr^{-1}) (Henze et al.

Table 3 Annual and seasonal estimates of background SOA for the SEUS compared to global SOA production values

	Measured background SOA production							
	Summer				Winter			
	SOA annual estimate (GgSOA yr^{-1})				SOA annual estimate (GgSOA yr^{-1})			
	Estimated SOA lifetime				Estimated SOA lifetime			
	4 days	5.4 days	8.1 days	11 days	4 days	5.4 days	8.1 days	11 days
[a]Measured PBL	0.56	0.41	0.28	0.20	0.47	0.35	0.23	0.17
[b]Estimated PBL	0.84	0.62	0.42	0.38	0.71	0.52	0.35	0.26
	SOC annual estimate (GgC yr^{-1})				SOC annual estimate (GgC yr^{-1})			
[a]Measured PBL	0.40	0.30	0.20	0.15	0.33	0.25	0.16	0.12
[b]Estimated PBL	0.60	0.45	0.30	0.22	0.50	0.37	0.25	0.18
	[c]Estimated background SOC in SEUS by season (GgC yr^{-1})							
	0.50	0.38	0.25	0.19	0.42	0.31	0.21	0.15
	[d]Annual Range (GgC yr^{-1})							
	Estimated SOA lifetime							
	4 days		5.4 days		8.1 days		11 days	
	0.42–0.5		0.31–0.38		0.21–0.25		0.15–0.19	
	[e]Global SOA production estimates from literature (GgC yr^{-1})							
	[*]4400	8600	[*]9300	21,100	40,000	88,000	[*]100,000	
	[f]Expected ratio of total SOA from SEUS based off land surface area ratio (GgC yr^{-1})							
	0.28	0.54	0.58	1.32	2.37	5.50	6.25	

[a] The measured PBL is 1590 m resulting from the average of the specific humidity method calculation

[b] The estimated PBL is 2400 m based off of observed OA column distributions from other studies (Morgan et al. 2009; Robinson et al. 2011) as well as maximum observed PBL values reported from other studies (Seidel et al. 2010)

[c] Each value is the resulting average between the measured PBL and estimated PBL SOC annual estimate values

[d] Estimated background SOC values for the summer and winter are used as the upper and lower bounds on the reported ranges, respectively

[e] Values presented here represent values reported for global SOA flux estimates from literature sources for; 4.4 TgC yr^{-1} (SOA from isoprene oxidation) (Henze and Seinfeld 2006), 8.6 TgC yr^{-1} (SOA formed from anthropogenic volatile precursors) (Henze et al. 2008), 9.3 TgC yr^{-1} (biogenic SOA) (Spracklen et al. 2011), 21.1 TgC yr^{-1} (terpenes+isoprene SOA) (Kanakidou et al. 2005), 88 TgC yr^{-1} (biogenic SOC) (Hallquist et al. 2009), and 100 TgC yr^{-1} (total global SOA) (Spracklen et al. 2011)

[f] Values presented here were calculated by multiplying the ratio of the productive surface area of the earth to the surface area of the SEUS by the global biogenic SOA production estimates provided from literature sources

[*] Values converted to TgC yr^{-1} from TgSOA yr^{-1} using OM/OC=1.4

2008). If the total average summertime OA concentration measured in this experiment is used as an approximate lower bound for total OC in the SEUS and average total OA summertime concentrations reported in another study (Budisulistiorini et al. 2013) from Atlanta GA is used as an upper bound for total OC in the SEUS, these calculations produce a total OC estimate range of 1.3–14 GgC yr^{-1} using an SOA lifetime of 5.4 days and PBL height of 2.4 km agl. This estimate is particularly uncertain and is only presented here to demonstrate that while calculated background production values fall within the lower bounds of the expected total reported SOA estimates, calculated total SOC for the SEUS has considerable potential to exceed the upper bound of what

might be expected for total SOC in the SEUS. This is consistent with the hypothesis that the SEUS is a significant source of SOA to the global SOA budget.

4 Conclusions

Aerosol and gas-phase chemical measurements were analyzed during the summer of 2013 to identify the primary influences on warm season atmospheric chemistry at a high elevation, rural site in the Appalachian mountains of North Carolina. Minimal direct urban influence was observed in both the aerosol and gas-phase chemical datasets. The dominance of an organic aerosol factor associated with isoprene IEPOX was observed during the summer sampling suggesting that reactions with acidic sulfate seed aerosol and isoprene BVOC emissions may have a significant influence on the total aerosol burden for the SEUS region. Though much of the observed patterns of chemical loading were statistically indistinguishable across different source regions, the IEPOX OA factor displayed patterns of loading that were statistically higher from the north and west than the other source regions. This suggests that these regions may be significant sources of anthropogenic sulfate aerosol and/or isoprene leading to the formation of this type of OA.

Results of analyses performed in this experiment suggest that AppalAIR is a site regionally representative of the SEUS suitable for estimating background SOA levels and observing background aerosol and VOC chemistry. Comparisons between the magnitudes of IEPOX-OA and the background OA observed in this study suggest that anthropogenic enhancement of SOA production in the SEUS may contribute to the total OA burden by a factor of two or more. Characterization of background SOA from other sites in the SEUS should be compared to the results from this study in order to further estimate the extent of anthropogenic influence on SOA production in the SEUS.

Acknowledgments Additional information and analyses performed in this study can be found in the supplemental information. Funding for this work was provided by the Appalachian Chemistry Research Experience in Energy and the Environment (NSF-REU CHE #1004896), Office of Student Research at Appalachian State University and the Chemistry Department at Appalachian State University. We thank all of the environmental science, physics, and chemistry students at Appalachian State University for helping with data collection and processing. The authors acknowledge the NOAA Air Resources Laboratory for use of the HYSPLIT model and meteorological data. MODIS AOD data used in this study was produced with the Giovanni online data system, developed and maintained by the NASA GES DISC. The authors would like to thank D.K. Farmer and Robert Swarthout for their valuable input in constructing this manuscript. We also acknowledge the MODIS mission scientists and associated NASA personnel for the production of the data used in this research effort.

Compliance with Ethics Requirements

Conflict of Interest Michael Link declares he has no conflict of interest.
Yong Zhou declares he has no conflict of interest.
James Sherman declares he has no conflict of interest.
Brett Taubman declares he has no conflict of interest.
Hadi Morrow declares he has no conflict of interest.
Matthew West declares he has no conflict of interest.
Ryan Cook declares he has no conflict of interest.
Luke Robertson declares he has no conflict of interest.
Justine Stocks declares she has no conflict of interest.
Barkley Sive declares he has no conflict of interest.
Ian Krintz declares he has no conflict of interest.

Animal or Human Subjects This article does not contain any studies with human or animal subjects.

References

Aiken, A.C., DeCarlo, P.F., Kroll, J.H., Worsnop, D.R., Huffman, J.A., Docherty, K.S., Ulbrich, I.M., Mohr, C., Kimmel, J.R., Sueper, D., Sun, Y., Zhang, Q., Trimborn, A., Northway, M., Ziemann, P.J., Canagaratna, M.R., Onasch, T.B., Alfarra, M.R., Prevot, A.S.H., Dommen, J., Duplissy, J., Metzger, A., Baltensperger, U., Jimenez, J.L.: O/C and OM/OC ratios of primary, secondary, and ambient organic aerosols with High-Resolution Time-of-Flight Aerosol Mass Spectrometry. Environ. Sci. Technol. **42**, 4478–4485 (2008)

Apel, E.C., Riemer, D.D., Hills, A., Baugh, W., Orlando, J., Faloona, I., Tan, D., Brune, W., Lamb, B., Westberg, H., Carroll, M.A., Thornberry, T., Geron, C.D.: Measurement and interpretation of isoprene fluxes and isoprene, methacrolein, and methyl vinyl ketone mixing ratios at the PROPHET site during the 1998 Intensive. J. Geophys. Res. **107**, 4034 (2002)

Baker, A.K., Beyersdorf, A.J., Doezema, L.A., Katzenstein, A., Meinardi, S., Simpson, I.J., Blake, D.R., Rowland, F.S.: Measurements of nonmethane hydrocarbons in 28 United States cities. Atmos. Environ. **42**, 170–182 (2008)

Blake, N.J., Blake, D.R., Sive, B.C., Katzenstein, A.S., Meinardi, S., Wingenter, O.W., Atlas, E.L., Flocke, F., Ridley, B.A., Sherwood Rowland, F.: The seasonal evolution of NMHCs and light alkyl nitrates at middle to high northern latitudes during TOPSE. J. Geophys. Res. **108**, 8359 (2003)

Bertin, N., Staudt, M., Hansen, U., Seufert, G., Ciccioli, P., Foster, P., Fugit, J.L., Torres, L.: Diurnal and seasonal course of monoterpene emissions from Quercus ilex (L.) under natural conditions–applications of light and temperature algorithms. Atmos. Environ. **31**, 135–144 (1997)

Bertman, S.B., Roberts, J.M., Parrish, D.D., Buhr, M.P., Goldan, P.D., Kuster, W.C., Fehsenfeld, F.C., Montzka, S.A., Westberg, H.: Evolution of alkyl nitrates with air-mass age. J. Geophys. Res. **100**, 22805–22813 (1995)

Brown, S.G., Lee, T., Norris, G.A., Roberts, P.T., Collett Jr., J.L., Paatero, P., Worsnop, D.R.: Receptor modeling of near-roadway aerosol mass spectrometer data in Las Vegas, Nevada, with EPA PMF. Atmos. Chem. Phys. Discuss. **11**, 22909–22950 (2011)

Budisulistiorini, S.H., Canagaratna, M.R., Croteau, P.L., Marth, W.J., Baumann, K., Edgerton, E.S., Shaw, S.L., Knipping, E.M., Worsnop, D.R., Jayne, J.T., Gold, A., Surratt, J.D.: Real-time continuous characterization of secondary organic aerosol derived from isoprene epoxydiols in downtown Atlanta, Georgia, using the Aerodyne Aerosol Chemical Speciation Monitor. Environ. Sci. Technol. **47**, 5686–5694 (2013)

Carlton, A.G., Baker, K.R.: Photochemical modeling of the Ozark isoprene volcano: MEGAN, BEIS, and their impacts on air quality predictions. Environ. Sci. Technol. **10**, 4438–4445 (2011)

Canagaratna, M.R., Jayne, J.T., Jimenez, J.L., Allan, J.D., Alfarra, M.R., Zhang, Q., Onasch, T.B., Drewnick, F., Coe, H., Middlebrook, A., Delia, A., Williams, L.R., Trimborn, A.M., Northway, M.J., DeCarlo, P.F., Kolb, C.E., Davidovits, P., Worsnop, D.R.: Chemical and microphysical characterization of ambient aerosols with the aerodyne aerosol mass spectrometer. Mass Spectrom. Rev. **26**, 185–222 (2007)

Claeys, M., Graham, B., Vas, G., Wang, W., Vermeylen, R., Pashynska, V., Cafmeyer, J., Guyon, P., Andreae, M.O., Artaxo, P., Maenhaut, W.: Formation of secondary organic aerosols through photooxidation of isoprene. Science **303**, 1173–1176 (2004)

Compton, J.C., Delgado, R., Berkoff, T.A., Hoff, R.M.: Determination of planetary boundary layer height on short spatial and temporal scales: a demonstration of the covariance wavelet transform in ground-based wind profiler and lidar measurements. J. Atmos. Ocean. Technol. **30**, 1556–1575 (2013)

Dindorf, T., Kuhn, U., Ganzeveld, L., Schebeske, G., Ciccioli, P., Holzke, C., Köble, R., Seufert, G., Kesselmeier, J.: Significant light and temperature dependent monoterpene emissions from European beech (Fagus sylvatica L.) and their potential impact on the European volatile organic compound budget. J. Geophys. Res. **111**, D16305 (2006)

Draxler, R.R.: HYSPLIT4 user's guide. NOAA Tech. Memo. ERL ARL-230, NOAA Air Resources Laboratory, Silver Spring, MD (1999)

Edgerton, E.S., Hopke, P.K., Kim, E.: Source identification of Atlanta aerosol by positive matrix factorization. J. Air Waste Manage. Assoc. **53**, 731–739 (2003)

Ford, B., Heald, C.L.: Aerosol loading in the Southeastern United States: reconciling surface and satellite observations. Atmos. Chem. Phys. Discuss. **13**, 9917–9952 (2013)

Galbally, I.E., Kirstine, W.: The production of methanol by flowering plants and the global cycle of methanol. J. Atmos. Chem. **43**, 195–229 (2002)

Gao, S., Surratt, J.D., Knipping, E.M., Edgerton, E.S., Shahgholi, M., Seinfeld, J.H.: Characterization of polar organic components in fine aerosols in the southeastern United States: identity, origin, and evolution. J. Geophys. Res. Atmos. **111**, D14 (2006)

Griffin, R.J., Crocker III, D.R., Dabdub, D., Seinfeld, J.H.: Estimate of global atmospheric organic aerosol from oxidation of biogenic hydrocarbons. Geophys. Res. Lett. **26**, 2721–2724 (1999)

Goldstein, A.H., Galbally, I.E.: Known and unexplored organic constituents in the earth's atmosphere. Environ. Sci. Technol. **41**, 1514–1521 (2007)

Goldstein, A.H., Koven, C.D., Heald, C.L., Fung, I.Y.: Biogenic carbon and anthropogenic pollutants combine to form a cooling haze over the southeastern United States. Proc. Natl. Acad. Sci. U. S. A. **106**, 8835–8840 (2009)

Hains, J.C., Taubman, B.F., Thompson, A.M., Stehr, J.W., Marufu, L.T., Doddridge, B.G., Dickerson, R.R.: Origins of chemical pollution derived from Mid-Atlantic aircraft profiles using a clustering technique. Atmos. Environ. **42**, 1727–1741 (2008)

Hallquist, M., Wenger, J.C., Baltensperger, U., Rudich, Y., Simpson, D., Claeys, M., Dommen, J., Donahue, N.M., George, C., Goldstein, A.H., Hamilton, J.H., Herrmann, H., Hoffmann, T., Iinuma, Y., Jang, M., Jenkin, M.E., Jimenez, J.L., Kiendler-Scharr, A., Maenhaut, W., McFiggans, G., Mentel, T.F., Monod, A., Prévôt, A.S.H., Seinfeld, J.H., Surratt, J.D., Szmigielski, R., Wildt, J.: The formation, properties and impact of secondary organic aerosol: current and emerging issues. Atmos. Chem. Phys. **9**, 5155–5236 (2009)

Heald, C.L., Jacob, D.J., Park, R.J., Russell, L.M., Huebert, B.J., Seinfeld, J.H., Liao, H., Weber, R.J.: A large organic aerosol source in the free troposphere missing from current models. Geophys. Res. Lett. **32**, LI8809 (2005)

Heald, C.L., Ridley, D.A., Kreidenweis, S.M., Drury, E.E.: Satellite observations cap the atmospheric organic aerosol budget. Geophys. Res. Lett. **37**, L24808 (2010)

Hansen, D.A., Edgerton, E.S., Hartsell, B.E., Jansen, J.J., Kandasamy, N., Hidy, G.M., Blanchard, C.L.: The Southeastern aerosol research and characterization study: part 1—overview. J. Air Waste Manag. Assoc. **53**, 1460–1471 (2003)

Henze, D.K., Seinfeld, J.H.: Global secondary organic aerosol from isoprene oxidation. Geophys. Res. Lett. **33**, L09812 (2006)

Henze, D.K., Seinfeld, J.H., Ng, N.L., Kroll, J.H., Fu, T.-M., Jacob, D.J., Heald, C.L.: Global modeling of secondary organic aerosol formation from aromatic hydrocarbons: high- vs. low-yield pathways. Atmos. Chem. Phys. **8**, 2405–2420 (2008)

Hoyle, C.R., Boy, M., Donahue, N.M., Fry, J.L., Glasius, M., Guenther, A., Hallar, A.G., Huff Hartz, K., Petters, M.D., Petäjä, T., Rosenoern, T., Sullivan, A.P.: A review of the anthropogenic influence on biogenic secondary organic aerosol. Atmos. Chem. Phys. **11**, 321–343 (2011)

Huffman, J.A., Docherty, K.S., Aiken, A.C., Cubison, M.J., Ulbrich, I.M., DeCarlo, P.F., Sueper, D., Jayne, J.T., Worsnop, D.R., Ziemann, P.J., Jimenez, J.L.: Chemically-resolved aerosol volatility measurements from two megacity field studies. Atmos. Chem. Phys. **9**, 7161–7182 (2009)

IPCC, 2013: Climate Change 2013: The Physical Science Basis. Contribution of Working Group I to the Fifth Assessment Report of the Intergovernmental Panel on Climate Change. In: Stocker, T.F., Qin, D., Plattner, G.-K., Tignor, M., Allen, S.K., Boschung, J., Nauels, A., Xia, Y., Bex V., P.M., Midgley (eds.). Cambridge University Press, Cambridge, 1535 (2013)

Jayne, J.T., Leard, D.C., Zhang, X., Davidovits, P., Smith, K.A., Kolb, C.E., Worsnop, D.R.: Development of an aerosol mass spectrometer for size and composition analysis of submicron particles. Aerosol Sci. Technol. **33**, 49–70 (2000)

Jimenez, J.L., Jayne, J.T., Shi, Q., Kolb, C.E., Worsnop, D.R., Yourshaw, I., Seinfeld, J.H., Flagan, R.C., Zhang, X., Smith, K.A., Morris, J.W., Davidovits, P.: Ambient aerosol sampling with an aerodyne aerosol mass spectrometer. J. Geophys. Res. **108**, 8425 (2003)

Jimenez, J.L., Canagaratna, M.R., Donahue, N.M., Prevot, A.S.H., Zhang, Q., Kroll, J.H., DeCarlo, P.F., Allan, J.D., Coe, H., Ng, N.L., Aiken, A.C., Docherty, K.S., Ulbrich, I.M., Grieshop, A.P., Robinson, A.L., Duplissy, J., Smith, J.D., Wilson, K.R., Lanz, V.A., Hueglin, C., Sun, Y.L., Tian, J., Laaksonen, A., Raatikainen, T., Rautiainen, J., Vaattovaara, P., Ehn, M., Kulmala, M., Tomlinson, J.M., Collins, D.R., Cubison, M.J., Dunlea, E.J., Huffman, J.A., Onasch, T.B., Alfarra, M.R., Williams, P.I., Bower, K., Kondo, Y., Schneider, J., Drewnick, F., Borrmann, S., Weimer, S., Demerjian, K., Salcedo, D., Cottrell, L., Griffin, R., Takami, A., Miyoshi, T., Hatakeyama, S., Shimono, A., Sun, J.Y., Zhang, Y.M., Dzepina, K., Kimmel, J.R., Sueper, D., Jayne, J.T., Herndon, S.C., Trimborn, A.M., Williams, L.R., Wood, E.C., Middlebrook, A.M., Kolb, C.E., Baltensperger, U., Worsnop, D.R.: Evolution of organic aerosols in the atmosphere. Science **326**, 1525 (2009)

Jordan, C., Fitz, E., Hagan, T., Sive, B., Frinak, E., Haase, K., Cottrell, L., Buckley, S., Talbot, R.: Long-term study of VOCs measured with PTR-MS at a rural site in New Hampshire with urban influences. Atmos. Chem. Phys. **9**, 4677–4697 (2009)

Kanakidou, M., Seinfeld, J.H., Pandis, S.N., Barnes, I., Dentener, F.J., Facchini, M.C., Van Dingenen, R., Ervens, B., Nenes, A., Nielsen, C.J., Swietlicki, E., Putaud, J.P., Balkanski, Y., Fuzzi, S., Horth, J., Moortgat, G.K., Winterhalter, R., Myhre, C.E.L., Tsigaridis, K., Vignati, E., Stephanou, E.G., Wilson, J.: Organic aerosol and global climate modelling: a review. Atmos. Chem. Phys. **5**, 1053–1123 (2005)

Kang, D., Aneja, V.P., Mathur, R., Ray, J.D.: Nonmethane hydrocarbons and ozone in three rural southeast United States national parks: a model sensitivity analysis and comparison to measurements. J. Geophys. Res. **108**, 4604 (2003)

Karl, T., Guenther, A., Spirig, C., Hansel, A., Fall, R.: Seasonal variation of biogenic VOC emissions above a mixed hardwood forest in northern Michigan. Geophys. Res. Lett. **30**, 2186 (2003)

Kelly, G., Perry, B., Taubman, B., Soulè, P.: Synoptic classification of precipitation events in the Southern Appalachian Mountains. Clim. Res. **55**, 1–15 (2012)

Kesselmeier, J., Staudt, M.: Biogenic volatile organic compounds (VOC): an overview on emission, physiology and ecology. J. Atmos. Chem. **33**, 23–88 (1999)

Lanz, V.A., Alfarra, M.R., Baltensperger, U., Buchmann, B., Hueglin, C., Prévôt, A.S.H.: Source apportionment of submicron organic aerosols at an urban site by factor analytical modelling of aerosol mass spectra. Atmos. Chem. Phys. **7**, 1503–1522 (2007)

Liao, H., Henze, D.K., Seinfeld, J.H., Wu, S., Mickley, L.J.: Biogenic secondary organic aerosol over the United States: comparison of climatological simulations with observations. J. Geophys. Res. **112**, D06201 (2007)

Lin, Y.H., Zhang, H., Pye, H.O., Zhang, Z., Marth, W.J., Park, S., Arashiro, M., Cui, T., Budisulistiorini, S.H., Sexton, K.G., Vizuete, W., Xie, Y., Luecken, D.J., Piletic, I.R., Edney, E.O., Bartolotti, L.J., Gold, A., Surratt, J.D.: Epoxide as a precursor to secondary organic aerosol formation from isoprene photooxidation in the presence of nitrogen oxides. Proc. Natl. Acad. Sci. **110**, 6718–6723 (2013)

Liousse, C., Penner, J.E., Chuang, C., Walton, J.J., Eddieman, H., Cachier, H.: A global three-dimensional model study of carbonaceous aerosols. J. Geophys. Res. **101**, 19411–19432 (1996)

Liu, P., Ziemann, P.J., Kittelson, D.B., McMurry, P.H.: Generating particle beams of controlled dimensions and divergence: I. Theory of particle motion in aerodynamic lenses and nozzle expansions. Aerosol Sci. Technol. **22**, 293–313 (1995a)

Liu, P., Ziemann, P.J., Kittelson, D.B., McMurry, P.H.: Generating particle beams of controlled dimensions and divergence: II. Experimental evaluation of particle motion in aerodynamic lenses and nozzle expansions. Aerosol Sci. Technol. **22**, 314–324 (1995b)

Mao, H., Talbot, R., Nielsen, C., Sive, B.C.: Controls on methanol and acetone in marine and continental atmospheres. Geophys. Res. Lett. **33**, L02803 (2006)

Morgan, W.T., Allan, J.D., Bower, K.N., Capes, G., Crosier, J., Williams, P.I., Coe, H.: Vertical distribution of sub-micron aerosol chemical composition from North-Western Europe and the North-East Atlantic. Atmos. Chem. Phys. **9**, 5389–5401 (2009)

Ng, N.L., Canagaratna, M.R., Zhang, Q., Jimenez, J.L., Tian, J., Ulbrich, I.M., Kroll, J.H., Docherty, K.S., Chhabra, P.S., Bahreini, R., Murphy, S.M., Seinfeld, J.H., Hildebrandt, L., Donahue, N.M., DeCarlo, P.F., Lanz, V.A., Prévôt, A.S.H., Dinar, E., Rudich, Y., Worsnop, D.R.: Organic aerosol components observed in Northern Hemispheric datasets from Aerosol Mass Spectrometry. Atmos. Chem. Phys. **10**, 4625–4641 (2010)

Paatero, P., Tapper, U.: Positive Matrix Factorization – a nonnegative factor model with optimal utilization of error-estimates of data values. Environmetrics **5**, 111–126 (1994)

Paatero, P.: The multilinear engine - A table-driven, least squares program for solving multilinear problems, including the n-way parallel factor analysis model. J. Comput. Graph. Stat. **8**, 854–888 (1999)

Pye, H.O.T., Pinder, R.W., Piletic, I.R., Xie, Y., Capps, S.L., Lin, Y.-H.S., Surratt, J.D., Zhang, Z., Gold, A., Luecken, D.J., Hutzell, W.T., Jaoui, M., Offenberg, J.H., Kleindienst, T.E., Lewandowski, M., Edney, E.O.: Epoxide pathways improve model predictions of isoprene markers and reveal key role of acidity in aerosol formation. Environ. Sci. Technol. **47**, 11056–11064 (2013)

Riemer, D., Pos, W., Milne, P., Farmer, C., Zika, R., Apel, E., Olszyna, K., Kliendienst, T., Lonneman, W., Bertman, S., Shepson, P., Starn, T.: Observations of nonmethane hydrocarbons and oxygenated volatile organic compounds at a rural site in the southeastern United States. J. Geophys. Res. **103**, 28111–28128 (1998)

Robinson, N.H., Hamilton, J.F., Allan, J.D., Langford, B., Oram, D.E., Chen, Q., Docherty, K., Farmer, D.K., Jimenez, J.L., Ward, M.W., Hewitt, C.N., Barley, M.H., Jenkin, M.E., Rickard, A.R., Martin, S.T., McFiggans, G., Coe, H.: Evidence for a significant proportion of Secondary Organic Aerosol from isoprene above a maritime tropical forest. Atmos. Chem. Phys. **11**, 1039–1050 (2011)

Russo, R.S., Zhou, Y., White, M.L., Mao, H., Talbot, R., Sive, B.C.: Multi-year (2004–2008) record of nonmethane hydrocarbons and halocarbons in New England: seasonal variations and regional sources. Atmos. Chem. Phys. **10**, 4909–4929 (2010)

Schade, G.W., Goldstein, A.H.: Fluxes of oxygenated volatile organic compounds from a ponderosa pine plantation. J. Geo. Phys. Res. **106**, 3111–3123 (2001)

Schade, G.W., Goldstein, A.H.: Seasonal measurements of acetone and methanol: abundances and implications for atmospheric budgets. Global Biogeochem. Cycles **20**, GB1011 (2006)

Seinfeld, J.H., Pandis, S.N.: Atmospheric Chemistry and Physics: From Air Pollution to Climate Change, 2nd edn. Wiley, New York (2006)
Seidel, D.J., Ao, C.O., Li, K.: Estimating climatological planetary boundary layer heights from radiosonde observations: comparison of methods and uncertainty analysis. J. Geophys. Res. **115**, D16113 (2010)
Simpson, I.J., Meinardi, S., Blake, N.J., Rowland, F.S., Blake, D.R..: Long-term decrease in the global atmospheric burden of tetrachloroethene (C_2Cl_4). Geo. Phys. Res. Let. **31**, L08108 (2004)
Sive, B.C.: Atmospheric nonmethane hydrocarbons: analytical methods and estimated hydroxyl radical concentrations. Ph.D. thesis, Univ. of Calif., Irvine. (1998)
Slowik, J.G., Stroud, C., Bottenheim, J.W., Brickell, P.C., Chang, R.Y.-W., Liggio, J., Makar, P.A., Martin, R.V., Moran, M.D., Shantz, N.C., Sjostedt, S.J., van Donkelaar, A., Vlasenko, A., Wiebe, H.A., Xia, A.G., Zhang, J., Leaitch, W.R., Abbatt, J.P.D.: Characterization of a large biogenic secondary organic aerosol event from eastern Canadian forests. Atmos. Chem. Phys. **10**, 2825–2845 (2010)
Spracklen, D.V., Jimenez, J.L., Carslaw, K.S., Worsnop, D.R., Evans, M.J., Mann, G.W., Zhang, Q., Canagaratna, M.R., Allan, J., Coe, H., McFiggans, G., Rap, A., Forster, P.: Aerosol mass spectrometer constraint on the global secondary organic aerosol budget. Atmos. Chem. Phys. **11**, 12109–12136 (2011)
Surratt, J.D., Kroll, J.H., Kleindienst, T.E., Edney, E.O., Claeys, M., Sorooshian, A., Ng, N.L., Offenberg, J.H., Lewandowski, M., Jaoui, M., Flagan, R.C., Seinfeld, J.H.: Evidence for organosulfates in secondary organic aerosol. Environ. Sci. Technol. **41**, 517–527 (2007a)
Surratt, J.D., Lewandowski, M., Offenberg, J.H., Jaoui, M., Kleindienst, T.E., Edney, E.O., Seinfeld, J.H.: Effect of acidity on secondary organic aerosol formation from isoprene. Environ. Sci. Technol. **41**, 5363–5369 (2007b)
Surratt, J.D., Chan, A.W.H., Eddingsaas, N.C., Chan, M.N., Loza, C.L., Kwan, A.J., Hersey, S.P., Flagan, R.C., Wennberg, P.O., Seinfeld, J.H.: Reactive intermediates revealed in secondary organic aerosol formation from isoprene. Proc. Natl. Acad. Sci. **107**, 6640–6664 (2010)
Swanson, A.L., Blake, N.J., Atlas, E., Flocke, F., Blake, D.R., Rowland, F.S.: Seasonal variations of C2–C4 nonmethane hydrocarbons and C1–C4 alkyl nitrates at the Summit research station in Greenland. J. Geophys. Res. **108**, 4065 (2003)
Swarthout, R.F., Russo, R.S., Zhou, Y., Hart, A.H., Sive, B.C.: Volatile organic compound distributions during the NACHTT campaign at the Boulder Atmospheric Observatory: influence of urban and natural gas sources. J. Geo. Phys. Res. Atm. **118**, 614–610 (2013). **637**
Taubman, B.F., Hains, J.C., Thompson, A.M., Marufu, L.T., Doddridge, B.G., Stehr, J.W., Piety, C.A., Dickerson, R.R.: Aircraft vertical profiles of trace gas and aerosol pollution over the mid-Atlantic United States: statistics and meteorological cluster analysis. J. Geophys. Res. **111**, D10S07 (2006)
Tsigaridis, K., et al.: The AeroCom evaluation and intercomparison of organic aerosol in global models. Atmos. Chem. Phys. Discuss. **14**, 6027–6161 (2014)
Ulbrich, I.M., Canagaratna, M.R., Zhang, Q., Worsnop, D.R., Jimenez, J.L.: Interpretation of organic components from Positive Matrix Factorization of aerosol mass spectrometric data. Atmos. Chem. Phys. **9**, 2891–2918 (2009a)
Ulbrich, I.M., Lechner, M., Jimenez, J.L.: AMS Spectral Database. URL: http://cires.colorado.edu/jimenez-group/AMSsd/ (2009b). Accessed 14 Jan 2013
Volkamer, R., Jimenez, J.L., Dzepina, K., Salcedo, D., SanMartini, F.M., Molina, L.T., Worsnop, D.R., Molina, M.J.: Secondary organic aerosol formation from anthropogenic air pollution. Rapid and higher than expected. Geophys. Res. Lett. **33**, L17811 (2006)
White, M.L., Russo, R.S., Zhou, Y., Mao, H., Varner, R.K., Ambrose, J., Veres, P., Wingenter, O.W., Haase, K., Stutz, J., Talbot, R., Sive, B.C.: Volatile organic compounds in northern New England marine and continental environments during the ICARTT 2004 campaign, J. Geophys. Res. **113**, D08S90 (2008)
Zhang, Q. et al.: Ubiquity and dominance of oxygenated species in organic aerosols in anthropogenically-influenced Northern Hemisphere midlatitudes. Geophys. Res. Lett. **34**, L13801 (2007a)
Zhang, Y., Huang, J.-P., Henze, D.K., Seinfeld, J.H.: Role of isoprene in secondary organic aerosol formation on a regional scale. J. Geophys. Res. **112**, D20207 (2007b)
Zhang, Q., Jimenez, J.L., Canagaratna, M.R., Ulbrich, I.M., Ng, N.L., Worsnop, D.R., Sun, Y.L.: Understanding atmospheric organic aerosols via factor analysis of aerosol mass spectrometry a review. Anal. Bioanal. Chem. **401**, 3045–3067 (2011)
Zhou, Y., Varner, R.K., Russo, R.S., Wingenter, O.W., Haase, K.B., Talbot, R., Sive, B.C.: Coastal water source of short-lived halocarbons in New England. J. Geophys. Res. **110**, D21302 (2005)
Zhou, Y., Shively, D., Mao, H., Russo, R.S., Pape, B., Mower, R.N., Talbot, R., Sive, B.C.: Air toxic emissions from snowmobiles in Yellowstone National Park. Environ. Sci. Technol. **44**, 222–228 (2010)